On the orbital rehybridization in tetrahedral amorphous carbon

Aniekan Magnus Ukpong

Department of Physics, University of Pretoria, South Africa

aniekan.ukpong@up.ac.za

Abstract. The use of tetrahedral amorphous carbon thin films in bolometers depends strongly on the ability to tune its optical properties. This can be achieved by controlling the density of dangling bond defects and the disorder in the material. The pi-orbital axis vector theory is used in this study to investigate the phenomenon of rehybridization of the carbon bonding in tetrahedral amorphous carbon. It is shown that the correlated pi - pi* orbitals is locally entangled due to the competition between the on-site Coulomb interaction and the hybridization. A microscopic model is proposed for the reduction in strain in the material due to hydrogenation, based on the $sp^3 - sp^2$ conversion reaction. It is demonstrated that the activation energy for this conversion is dependent on the Urbach energy, and therefore on the disorder. The implication of the results on the manifestation of strain in similar, carbon-based, materials is discussed.

1. Introduction

Solid-state quantum information processing is only achievable if there is control of the properties of the functional material. One basic resource for controlling the electronic degrees of freedom in such systems is the quantum entanglement between electronic states [1-3]. Entanglement is a measure of the correlation in quantum mechanical systems. In the entangled state, the best possible knowledge of the whole system does not necessarily imply the best possible knowledge of its constituents [4]. Over the nearly eight decades since its introduction, the concept of quantum entanglement has significantly changed in meaning, and its nature and interpretation may still continue to change [5]. In this study, its interpretation in terms of the anisotropic coupling between atomic orbitals allows for the characterization and tunability of the physical properties of materials. This is directly applicable to the selection of suitable absorptive materials for bolometer applications. For instance, although amorphous silicon (a-Si) [6] or vanadium dioxide (VO_2) [7] films are the commonly used photo-responsive materials in bolometers operated within the infra-red/ultra-violet (IV/UV) range, other materials can equally be used. In particular, the use of tetrahedral amorphous carbon (ta-C) films in this role cannot be overruled due to fundamental similarities between the local network structures in carbon and silicon. This makes amorphous carbon films an attractive subject of fundamental investigation since the hybridization state of the carbon atoms is expected to play a fundamental role in determining the resulting physical properties [8]. In our recent molecular dynamics simulations of typical ta-C networks for instance, the network stress was found to relax in the presence of hydrogen although the exact mechanism remained unclear [9]. This paper clarifies the mechanism of stress relaxation in ta-C networks by investigating the role of hydrogen on stereo-electronic factors and the resulting physical properties of the material.

2. Theory and computations

First principles molecular dynamics calculations were performed to implement the melt-quenching procedure of simulating tetrahedral amorphous carbon (ta-C) from diamond-like carbon. The calculations were performed on a 64-atom supercell using the VASP electronic structure codes [10-13] This allows for self-consistent solutions to the Kohn-Sham equations using the projector augmented wave (PAW) method [14,15], and a plane wave basis set. Kinetic energy cutoff of 500 eV was used for expanding the plane wave basis set of the electron wave functions. Atomic positions were relaxed on the fly using forces derived from Hellman-Feynman theorem. The convergence limit of 10^{-3} eV per step was set for the determination of electronic energies. The network structures were relaxed until the forces reduced to 0.03 eV/Å in each case. Hydrogen atoms were selectively incorporated to the optimized ta-C structure to produce ta-C:H structures at saturation levels corresponding to 15, 30 45 and 60 at % H. These levels of hydrogen concentration were deliberately chosen to maintain consistency with the bulk structures generated in previous tight-binding molecular dynamics (TBMD) simulations using a 512-atom supercell [9]. The electronic structure was calculated within LDA, and the optoelectronic properties were investigated in terms of stimulated optical inter-band transitions. Level 1 [16] of the POAV theory was used within the σ-π orbital separability approximation to calculate effect of hydrogen on π-orbital curvature [17-20], and the rehybridization sp^{2+n}, where n characterizes the degree of the rehybridization [21,22].

3. Results

The effect of hydrogen on π-orbital curvature, mean bond strain, and the relative strengths of the π-π interaction are presented in Table 1. The errors bars quoted in Table 1 were determined as the standard error in the mean of ten repeated calculations of the same data. The strain in the hydrogenated networks is normalised to the strain in the hydrogen-free structure. The presence of a substantial fraction of sp^2-hybridzed bonds, even at 0% H, implies that a fraction of π-electrons will always be present in structure due to formation of localised domains of aromatic or aliphatic carbon chains depending on saturation level. Table 1 shows that the ta-C:H networks which contain low hydrogen concentrations are relatively highly strained. From the hydrogen/sp^2/sp^3 ternary phase diagram [8], such networks contain olefinic chains (ta-C:H) in which the sp^2-hybridised carbon sites tend to cluster. On the other hand, disordered carbon networks that contain high hydrogen concentrations exhibit significantly low strains and tend to contain aromatic carbon chains. Hence, the physical properties of amorphous carbon thin films are determined by the level of H-concentration in the networks. The average interaction between two π-orbitals in these structures was determined using resonance theory [23] for the 64-atom supercell. The dependence of the strength of the inter-orbital interaction $V_{pp\pi}(1)$ with changing levels of H-saturation is also shown in Table 1.

Table 1. The σ-bond strain, π-orbital curvature, curvature-induced rehybridization, and the strength of π-π interaction in ta C:H networks under different levels of hydrogen saturation.

H content (%)	Orbital mixing factor, k	Rehybridization, n	π-orbital curvature (θ^2)	π-π interaction (eV)	σ-bond strain
0	0.61 ± 0.01	0.62 ± 0.01	0.69 ± 0.10	-1.55 ± 0.02	1.00 ± 0.02
15	0.40 ± 0.04	0.54 ± 0.03	0.84 ± 0.08	-1.83 ± 0.03	0.79 ± 0.05
30	0.33 ± 0.05	0.43 ± 0.02	1.06 ± 0.12	-2.03 ± 0.05	0.52 ± 0.01
45	0.27 ± 0.02	0.32 ± 0.01	1.17 ± 0.10	-2.57 ± 0.01	0.32 ± 0.03
60	0.20 ± 0.03	0.29 ± 0.02	1.22 ± 0.05	-3.06 ± 0.12	0.18 ± 0.02

Figure 1 shows the angular momentum resolved density of states (DOS). The Fermi level is aligned to correspond to 0 eV. As shown in Fig. 1(a), the *s*-orbital states in ta-C structures containing 0 and 15% H are dominated by valence band states. The number of conduction band states in the interval 0 - 5.0 eV is reduced when the structure is saturated with 15% hydrogen. Though not shown

explicitly, this effect is also observed for higher hydrogen concentrations. Figure 1(b) shows the π-electron density of states at different hydrogen saturation levels. The $1s$ state of H induces the perturbation of the valence band states in this case, even though it is not a core state. The DOS profiles show significant perturbations as the level of H saturation changes. The effect of the perturbation on the valence band results in the promotion of valence electron states into to the conduction band as more hydrogen is incorporated. This effect is mostly seen at valence band energies above -15 eV. A comparison of the conduction band states between 0 and 5 eV for structures containing 0 and 60 at. % H shows that the number of electron states is neither increased nor decreased even after saturation with 60% H. The number of valence band states within this energy interval is depleted. The π-electron DOS predicts metallic ta-C:H systems while the s-state resolved DOS gives an opposing effect at all levels of hydrogen saturation. The relative reduction in the density of bonding states (denoted as π-orbitals) at different levels of H-saturation, and the relative changes in the corresponding density of anti-bonding states (denoted as π*-orbitals) suggests that an anisotropic coupling exists between the π-orbitals.
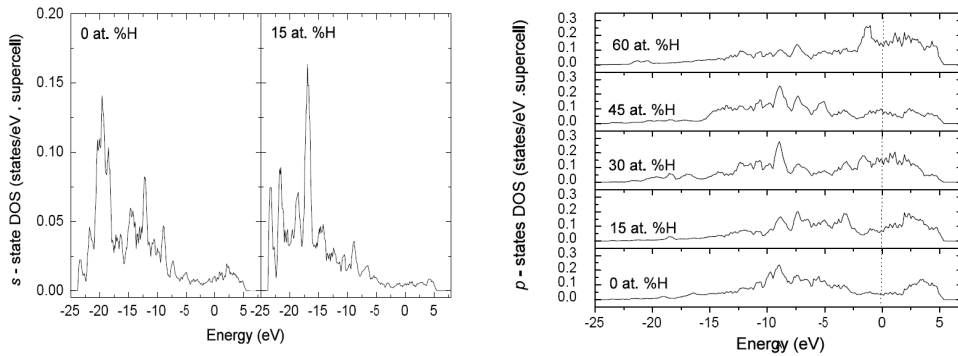

Figure 1. s-orbital electron states contribution to the density of states in ta-C structures containing 0 and 15 at. % H concentration (a), and π-orbital electron states contribution to the density of states in ta-C structures containing 0, 15, 30, 45 and 60 at. % H concentration (b).

In terms of the quantum nonseparability paradigm [24, 25], the anisotropic coupling indicates the local entanglement of the π-orbitals. The bonding (π) and anti-bonding (π*) states are simultaneously influenced by H-saturation irrespective of the concentration level. Figure 2(a) shows the total density of states for ta-C structures, which contain 0, 30 and 60 at. % H. The dynamical transfer of spectral weights from the s- and p-electron states to the total density of states is therefore crucial in maintaining the semiconducting state expected in ta-C:H materials. Hence, the dynamics of the entangled system was further investigated by treating the orbital mixing parameter as an anisotropic coupling constant to measures the evolution of orbital curvature and the degree of rehybridization as a function of H-saturation. Optical inter-band transitions may occur in ta-C:H due to excitation from extended to localized states and vice versa. In Figure 2(a), the conduction and valence band tails decay exponentially into the band gap. These Urbach-like band tails [26] suggest that the optical transitions in ta-C:H materials can be described with the exponential relationship of the form $\alpha(E) \sim \exp(\frac{E}{U_E})$ between absorption coefficient α and the photon energy E, where U_E is the Urbach energy [27]. The Urbach energy directly relates the degree of topological disorder in the material to its photoconductive properties. Figure 2(b) shows the dependence of Urbach energy on the sp^3-site faction in ta-C:H networks. The Urbach energy increases with increasing sp^3 site fraction and reaches a maximum when the sp^3 fraction is ~62 %. Further increases in the sp^3 site fraction beyond this point results in a steady decreases in Urbach energy. The sp^3 site fraction in ta-C:H decreases with increasing H-saturation [9]. The corresponding increase in second neighbour positional disorder with increasing H-content implies that sp^2/sp^3 ratio scales with the Urbach energy. The variation of U_E with sp^3-content shows an approximate linear relationship up to 60%. The present LDA calculations show that the Urbach energy

saturates at a slightly lower sp^3-site fraction compared to the 65% predicted in the empirical tight binding calculations of Mathioudakis *et al.* [28]. Nevertheless, the agreement between these two fundamentally dissimilar calculations - calculations performed within the local density approximation to density functional theory and those based on environment-dependent tight-binding (EDTB) method - shows that the physical and chemical properties of C-based materials are accurately described within phenomenological potentials.
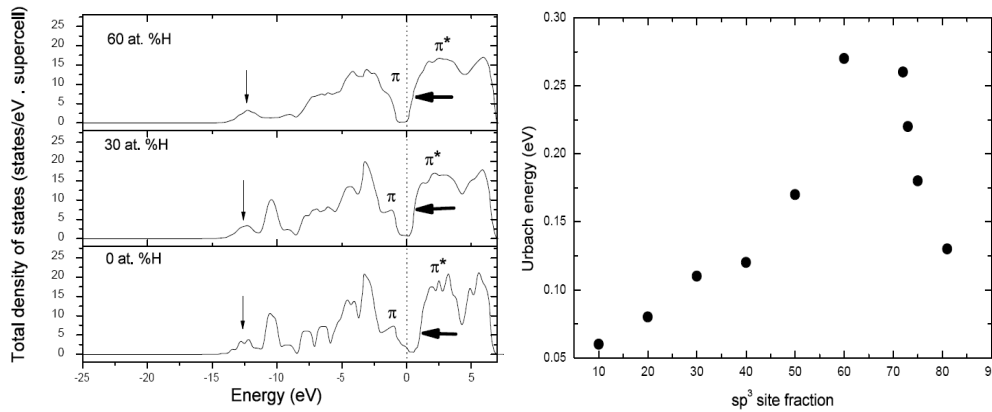

Figure 2. The total density of states in ta-C:H structures containing 0, 30 and 60 at. % H concentration showing the effect of hydrogen saturation level on the π-bonding and π^* anti-bonding electron states.

Results of isothermal annealing experiments do not show any changes in the local bonding structure of *ta*-C:H materials below 600 °C [29]. This indicates that the $sp^3 \rightarrow sp^2$ bond conversion reaction does not pass through a transitional (or intermediate) reaction phase once it is activated. It is therefore assumed that the observed changes in local bonding structure in Fig. 2(b) can be modelled using the first-order reaction kinetics. Numerical modelling of the hydrogen dynamics as a random walk to simulate the structural evolution with temperature shows activated hydrogen dynamics at temperatures between 570 K and 1180 K. This observation agrees with the experimentally observed deuterium diffusion in ta-C and a-C films [30]. The diffusivity of hydrogen is 0.018 ($\pm$ 0.002) cm^2/s at 600 K. From this simulation, the activation energy for the hydrogen diffusion was derived based on the assumption of Arrhenius-like diffusion. The activation energy was obtained by plotting the hydrogen diffusion coefficient against the simulated annealing temperature as shown in Fig. 3. An interpolation of the temperature and H-content that yields the maximum sp^3 site-fraction of 62% and Urbach energy U_E of Fig. 2(b) gives the activation energy as $\Delta H = 1.14$ meV for the bond conversion reaction.

$$D = D_0 \exp(\Delta H / kT)$$
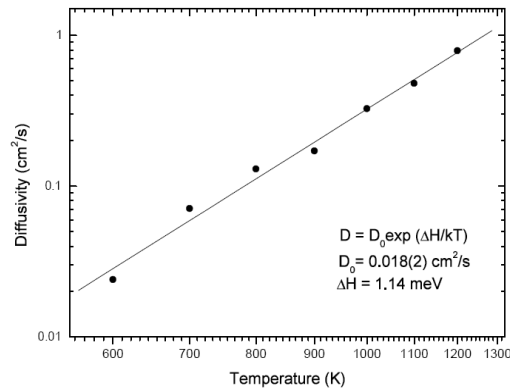$$D_0 = 0.018(2) \ cm^2/s$$
$$\Delta H = 1.14 \ meV$$

Figure 3. Arrhenius plot of H diffusion coefficient as a function of temperature on a logaritmic scale. The straight line indicates the best-fit trendline between ln$D$ and the inverse temperature $1/kT$.

4. Discussion

The π-orbital curvature is generally small in ta-C:H materials but its effect on orbital rehybridization is nontrivial. The curvature varies within the range $0.84 < \theta < 1.87$ under the influence of H-saturation. It is found that the degree of rehybridization decreases rapidly towards a limiting value of 0.3 as the levels of H concentration is increased. The saturation of the rehybridization n at a small, non-zero, value at 60 % H content indicates that full graphitic sp^2-bonding is unachievable by hydrogenation alone. In addition, the magnitude of the π-orbital curvature saturates at a limiting value of 1.27 at high H-saturation limit. However, irrespective of relative orientations of π-orbitals, the local geometries of C-clusters only achieve full closures when the π-orbital curvature is 2.42. Such local geometries are only found in Buckminster fullerenes such as C_{60}, carbon nanotubes, and cyclic hydrocarbons where the conservation of curvature is well known [11]. Schmalz *et al*. [14] showed that in such curved C-structures, the strain on the σ-bonds scales linearly with orbital curvature and the π-orbital rehybridization n. The strain in the ta-C:H structures exhibit similar behaviour, and are therefore considered to arise from deviations from planar graphitic geometry due to misorientation of some π-orbitals, and due to the σ-orbitals being oriented in the tangential direction to the planar surface. The imperfect alignment of pairs of bond-forming orbitals leads to the rehybridization of the π-orbitals. The rehybridization is necessary to bring the two nearby orbitals into closer alignment. The analysis of the role of H in increasing the π-orbital curvature in ta-C:H is based on the assumption that planar graphite layer ($\theta = 0$) is strain-free. The evolution of bond strain in the ta-C:H structures has been gauged relative the graphite surface.

The $1s$ state of hydrogen is found to induce the entanglement of π-electron states by introducing the nonlocal correlation between the π-bonding and anti-bonding state. By locally switching on the inter-orbital interactions $Vpp\pi(1)$, we have explicitly included the effects of the on-site Coulomb interactions between electrons on two interacting π-orbitals. The inter-orbital interaction must therefore be in competition with the strength of the local hybridization of the local carbon bonding in order to maintain the semiconducting state in ta-C:H. Due to the local π-orbital entanglement, further saturation with hydrogen does not lead to appreciable increases in the number of conduction band states. The correlated nature of the bonding (π) and (π*) electron states arises due to the local competition between inter-orbital interactions and sp^{2+n} hybridization. As seen in the total electronic density of states, the effect of the $1s$ state of hydrogen on the carbon bonding and anti-bonding orbital is non-negligible. The total density of states shows that π* (anti-bonding) electron states in the bottom of the conduction band are effectively shifted towards lower energies as the concentration of hydrogen increases. Although defect-induced mid-gap levels are substantially eliminated upon H-saturation, the downward shift in the energy levels leads to substantially reduced energy gaps as H-content increases giving rise to the observed exponential conduction and valence band tails.

The changes in π-orbital curvature and the rehybridization and corresponding reduction in bond strain, shown in Table 1, suggest that the experimentally observed bond conversion reaction above 600 °C [29] is consistent with the systematic increase in orbital coupling constant. The total H-content in typical thin films depends on the deposition temperature and the amount of bonded-hydrogen reduces when the annealing temperature is high enough to induce spontaneous hydrogen diffusion. The H-evolution can be determined experimentally by characterizing the post-annealing hydrogen content in a thin film after annealing using materials characterization techniques such as nuclear reaction profiling or IR spectroscopy. It therefore follows as corollary that the observed bond conversion is denoted by the continuous decrease (and increase) in sp^3 (and sp^2) site-fraction as the hydrogen saturation level increases. Since the rehybridization necessary to reduce strain also depends on the concentration of hydrogen, it is argued that the activation energy of the $sp^3 \rightarrow sp^2$ bond conversion must also depend on the residual network disorder at the onset of the reaction, and therefore on the Urbach energy.

5. Conclusion

The π-orbital axis vector theory has been applied to the study of the changes in ta-C:H networks under variable H-saturation levels. The mechanism of hydrogen-mediated curvature-induced rehybridization of π-orbitals is found to lead to the relaxation of strain in the material. From the analysis of the orbital-resolved density of states, it is found that the bonding (π) and anti-bonding (π*) electronic states are locally entangled. The correlated nature of the π-orbitals is interpreted in terms of the anisotropic coupling of atomic orbitals, and shown to occur due to competition between the on-site, inter-orbital, Coulomb-like interaction and the orbital hybridization of the carbon atoms. Using simulated inter-band optical transitions, the total density of states, and the orbital rehybridization, the activation of the observed $sp^3 \rightarrow sp^2$ bond conversion is shown to depend on the residual network disorder and therefore on the Urbach energy.

References

[1]   Huang Z and Kais S 2005 *Chem. Phys. Lett*. **413** 1
[2]   Samuelsson P and Verdozzi C 2007 *Phys. Rev. B* **75** 132405
[3]   Craco L 2008 *Phys. Rev. B* **77** 125122
[4]   Schrödinger E 1935 *Naturwissenschaften* **23** 807
[5]   Bruß D 2002 *J. Math. Phys*. **43** 4237
[6]   Liu X M, Fang H J and Liu L T 2007 *Microelectronics Journal* **38** 735
[7]   Rajendra Kumar R T, Karunagaran B, Mangalaraj D, Narayandass S K, Manoravi P, Joseph M, Gopal V, Madaria R K and Sing J P 2003 *Mat. Res. Bull* **38** 1235
[8]   Robertson J 2002 *Mat. Sci. and Eng*. R **37** 129
[9]   Ukpong A M 2010 *Molecular Physics* **108** 1607
[10]   Kresse G and Hafner J 1993 *Phys. Rev*. B **47** 558
[11]   Kresse G and Hafner J 1994 *Phys. Rev*. B **49** 14251
[12]   Kresse G and Furthmuller J 1996 *Phys. Rev*. B **54** 11169
[13]   Kresse G and Furthmuller J 1996 *Comput. Mater. Sci*. **6** 11169
[14]   Blochl P E 1994 *Phys. Rev*. B **50** 17953
[15]   Kresse G and Joubert J 1999 *Phys. Rev*. B **59** 1758
[16]   Haddon R C 1987 *J. Phys. Chem*. **91** 3719
[17]   Haddon R C 1988 *Acc. Chem. Res*. **21** 243
[18]   Haddon R C 1993 *Science* **261** 1545
[19]   Haddon R C 1986 *Chem. Phys. Lett*. **125** 231
[20]   Schmalz T G, Seitz W A, Klein D J, and Hite G E 1988 *J. Am. Chem. Soc*. **110** 1113
[21]   Kleiner A and Eggert S 2001 *Phys. Rev*. B **64** 113402
[22]   Yu O, Jing-Cui P, Hui W and Zhi-Hua P 2008 *Chinese Physics* B **17** 1674
[23]   Harrison W A 1989 *Electronic structure and the properties of solids: the physics of the chemical bond* (New York: Dover)
[24]   Miller W H 1976 *Acc. Chem. Res*. **9** 306
[25]   Healey R 2009 *Holism and nonseparability in physics*, ed E N Zalta (Stanford: Encyclopedia of Philosophy)
[26]   Pan Y, Inam F, Zhang M and Drabold D A 2008 *Phys. Rev. Lett*. **100** 206403
[27]   Fanchini G and Tagliaferro A 2004 *Diam. Relat. Mater* **13** 1402
[28]   Mathioudakis C, Kopidakis G, Patsalas P and Kelires P C 2007 *Diam. Relat. Mater* **16** 1788
[29]   Grierson D S, Sumant A V, Konicek A R, Friedmann T A, Sullivan J P and Carpick R W 2010 *J. Appl. Phys.* **107** 033523
[30]   Kröger H, Ronning C, Hofsäss H, Neumaier P, Bergmaier A, Görgens L and Dollinger G 2003 *Diam. Relat. Mater* **12** 2042